EFFECT OF PRESSURIZATION ON TIP LEAKAGE LOSSES IN MICRO-SCALE CENTRIFUGAL COMPRESSORS

Andrés Sebastián - Rubén Abbas - Manuel Valdés*

Universidad Politécnica de Madrid (UPM)
José Gutiérrez Abascal 2, 28006 Madrid (Spain)
*andres.sebastian@upm.es

ABSTRACT

One of the main sources of efficiency losses in miniaturized turbomachinery is caused by their large relative tip clearances. These small turbomachines are gaining in importance in a number of novel energy systems working with different fluids at closed-loop conditions. The aim of this study is to analyze the effect of pressurization on these tip clearance losses. Both analytical and numerical methods are proposed for their characterization on a reference high-speed miniature radial compressor. Results show the effect of pressurization using four selected working fluids (air, carbon dioxide, propane and isobutane) with inlet pressures in the range of 1-4 bar. While only slight differences in clearance mass flow ratio are found between analytical and numerical approaches, the expected reduction in efficiency provided by the analytical method is not aligned to the numerical results. However, both methods agree in the fact that inlet pressure has low influence on the internal efficiency for all the working fluids simulated.

KEYWORDS

MICRO-TURBOMACHINERY, TIP LEAKAGE LOSSES, MINIATURIZATION, NON-CONVENTIONAL WORKING FLUIDS, INLET PRESSURIZATION

NOMENCLATURE

a	Speed of sound (m/s)
b_2	Impeller tip width (m)
c	Absolute velocity (m/s)
C_{ref}	Dietmann and Casey coef. (-)
c_f	Friction coefficient (-)
D	Characteristic diameter (m)
h	Specific enthalpy (kJ/kg)
L	Characteristic length (m)
$\dot{m}$	Mass flow (kg/s)
Ma	Mach number (-)
N	Rotational speed (min^{-1})
r	Radius (m)
Re	Reynolds-number (-)
s_{cl}	Clearance gap (m)
u	Blade velocity (m/s)
w	Relative velocity (m/s)
Z	Number of blades (#)
ρ	Density (kg/m^3)
η	Efficiency (-)
Φ	Flow coefficient (-)
χ	Mass flow ratio (-)
$\bar{\omega}$	Total pressure loss coef.

Subscripts

$0x$	total/stagnation conditions
1	impeller inlet
2	impeller outlet
3	diffuser outlet
cl	clearance
h	hub
n	normal
t	tip

Superscripts

$*$	homologous conditions
$'$	effective conditions
lm, ls	main/splitter blade leading edge
tm, ts	main/splitter blade trailing edge

INTRODUCTION

The current research and development of ultra-high-speed miniaturized turbocompressors is leading to expand their use in different novel applications. These micro-scale centrifugal compressors (MSCC), characterized by impeller sizes below 30 mm and rotational speeds above 200 kmin^{-1} (Casey et al., 2013), are increasingly present in new designs of heat pumps (Demierre et al., 2012), power systems (Zhao et al., 2012), trigeneration concepts (Sebastián et al., 2021) or even in the propulsion sector (İlhan et al., 2019). Some of these new applications propose the use of MSCCs for the compression of non-conventional fluids different from air such as refrigerant vapors, hydrocarbons, hydrogen or carbon dioxide. This allows to devise pressurized closed-loop cycles where the low pressure line value is above the atmospheric pressure. Since down-scaling implies low inlet Reynolds-number (Re), the use of pressurized fluids entails beneficial effects on the machine internal efficiency due to the increase in Reynolds-number within a laminar-to-turbulent regime.

One of the main challenges in micro-turbomachinery is the large relative tip clearances due to assembly and manufacturing tolerances. These large clearance ratios lead to increased tip leakage losses that limit drastically the efficiency in the considered reduced-scale compressors. This phenomenon has motivated recent works of several authors such as Wang et al. (2011) or Kim et al. (2016) who studied these effects on impeller tip variation including its deformation caused by the thermal load. Meanwhile, Jaatinen-Värri et al. (2016) characterized the presence of reversed flow into the impeller due to tip clearances increase. Similarly, Diehl et al. (2020) conducted an scaling investigation of these effects on a wide range of clearance ratios in a micro-scale compressor operating with R134a.

While the aforementioned pressurization of alternative working fluids may offer beneficial effects due to the reduction of viscous friction, an increase in the absolute pressure difference between the pressure and suction sides of the blade also takes place if the compression ratio is maintained. This trade-off has lead the authors to quantify the effect of inlet pressure on the tip leakage losses in micro-scale centrifugal compressors using carbon dioxide, propane and isobutane apart from air. These fluids have been previously assessed as good candidates for miniature power and cooling systems with inlet pressures in the range of 1-4 bar using a 21 mm impeller size MSCC (Valdés et al., 2018).

Therefore, the present work proposes the assessment of the tip leakage losses by means of both analytical and numerical approaches. First, new operating conditions when using different working fluids are calculated considering the corresponding corrections due to Reynolds-number effects. Then, one-dimensional phenomenological methods available in the literature are applied to estimate the expected losses variations and tip leakage mass flow rate when the fluid is changed and the inlet pressure increases. A numerical model of the impeller-diffuser of a reference micro-compressor stage is developed in order to characterize the complex three-dimensional interactions within the tip leakage phenomena. The results section shows these effects comparing both analytical and numerical methods.

OFF-DESIGN OPERATING CONDITIONS CALCULATION

The inlet operating conditions for the assessment of tip leakage losses when using different pressurized working fluids have been obtained by means of dimensional analysis. In addition, corresponding Reynolds-number corrections require to be applied since this study is particularized for micro-scale radial compressors. Taking as reference the off-design performance supplied by the manufacturer when using atmospheric air, the speedline-to-speedline Re-corrected homologous conditions can be calculated when using the considered pressurized working fluids: carbon dioxide, propane and isobutane.

Rotational speed (N) and mass flow rate ($\dot{m}$) are the control variables which determine the compressor performance. Homologous conditions when the fluid or inlet pressure are varied can be assessed if dynamical similarity is fulfilled for a given geometry. Hence, the equivalent rotational speed is obtained (Eq. 1) keeping constant the blade Mach number (ND/a_{01}). Similarly, mass flow ratio equivalence can be stated maintaining the flow Mach number ($\dot{m}/\rho_{01}a_{01}D^2$). However, the additional Reynolds-number effect on the flow coefficient due to the relative boundary layer increase needs to be taken into account. To that end, an empirical correction method proposed by Dietmann and Casey (2013) is considered. Equation 2 collects this Re-corrected homologous mass flow rate.

$$N^* = N\frac{a^*_{01}}{a_{01}} \tag{1}$$

$$\dot{m}^* = \dot{m}\frac{\rho^*_{01}a^*_{01}}{\rho_{01}a_{01}}\Big[1 - C_{ref}(\Phi)\frac{\Delta c_f}{c_{f,0}}\Big] \tag{2}$$

While the numerical approach only requires the control variables as input parameters, the use of phenomenological one-dimensional tip leakage correlations needs the prediction of the compressor off-design performance. Since the characteristic map is known for atmposheric air, the resultant total-to-total pressure ratio can be predicted by means of similitude keeping constant the head coefficient. Similarly, isentropic efficiency can be calculated using the aforementioned Re correction method. Regarding to the flow properties calculation, REFPROP database has been used considering real gas properties.

PHENOMENOLOGICAL TIP LEAKAGE CORRELATIONS

Reduced-order tip leakage correlations are generally extended within different sets of one-dimensional losses for predicting compressors performance. These correlations usually model a jet driven by the pressure difference between the pressure and suction side of the blade, assuming that its kinetic energy is lost due to mixing and vortex generation. Although the applicability of these methods to reduced-scale machines is not completely validated due to their large clearance ratios, they represent a phenomenological approximation to assess the effect of inlet pressurization. The two most widely used correlations have been suggested for this analysis.

The enthalpy loss correlation due to tip clearance proposed by Jansen (1967) is expressed in Eq. 3. It can be noted that the enthalpy loss variation is proportional to the relative clearance ratio (s_{cl}/b_2). Geometrical parameters such as the different radius or the effective number of blades (Z') are required.

$$\Delta h_{cl} = 0.6\frac{s_{cl}}{b_2}\sqrt{\frac{4\pi}{b_2 Z'}\Big(\frac{r^2_{1t} - r^2_{1h}}{(r_2 - r_{1t})(1 + \rho_2/\rho_1)}\Big)c_{u2}c_{m1}} \tag{3}$$

Meanwhile, Aungier (2000) proposes the characterization of tip leakage losses through the calculation of the pressure difference between the pressure and suction sides of the blade (Δp_{cl}) through Eq. 4. Resulting mass flow leakage ($\dot{m}_{cl}$) is then obtained assuming a velocity of this flow (u_{cl}) as if an abrupt contraction and expansion loss occurs when the flow enters and leaves the gap (Eq. 5). Aungier computes this loss in terms of a total pressure loss coefficient ($\bar{\omega}_{cl}$) in Eq. 6, which can be later transformed in terms of enthalpy loss.

$$\Delta p_{cl} = \frac{\dot{m}(r_2 c_{u2} - r_1 c_{u1})}{Z' \bar{r} \bar{b} L_B^{'}} \tag{4}$$

$$\dot{m}_{cl} = \rho_2 s_{cl} Z^{'} L_B^{'} u_{cl} \tag{5}$$

$$\bar{\omega}_{cl} = \frac{2\dot{m}_{cl}\Delta p_{cl}}{\dot{m}\rho_1 w_1^2} \tag{6}$$

NUMERICAL MODEL AND 3-D TIP LEAKAGE CHARACTERIZATION

The numerical model used in this work corresponds to a left-handed micro-scale centrifugal compressor which is being tested on a specifically designed test rig at *Universidad Politécnica de Madrid* facilities. Table 1 shows some characteristic data and key performance indicators at the design point (DP) using atmospheric air, where it can be also noted the large relative tip clearance (s_{cl}/b_2) considered.

Geometry data		**Performance at DP**	
Impeller hub diameter (mm)	6	Flow coefficient (-)	0.068
Impeller tip diameter (mm)	21	Head coefficient (-)	0.486
No. main/splitter blades (#)	7/7	Tip Mach number (-)	0.721
Relative tip clearance (-)	0.15	Chord Reynolds-number (-)	7.72×10^4
Tip width (mm)	1.4	Max. rotational speed (kmin^{-1})	280

Table 1: **Reference MSCC data and performance at design point (DP) using atmospheric air at 20°C.**

The software ANSYS 2019R2 has been used for the development of the model through its specific turbomachinery tools. The stage modeled is formed by a seventh part of the straight inlet duct, the impeller and the vaneless diffuser passage of the reference MSCC. Therefore, periodicity boundary conditions are required along with an inlet pressure and an outlet mass flow boundaries. Solid-to-fluid interfaces are set as adiabatic no-slip walls with smooth roughness. The meshing and grid processing have been conducted using Turbogrid. A 1.4 million cell reference mesh is obtained ensuring both a proper expansion ratio target and a correct near-wall treatment, especially in the clearance gap area. The grid-insensitive results assurance has been guaranteed by means of comparing the grid convergence index (GCI) to both a coarse (0.6 million cells) and a fine (3.1 millions cells) mesh. GCIs from intermediate to fine mesh have been obtained for the model key outputs (isentropic efficiency and pressure ratio) leading to 0.09% and 0.15% respectively. These values give an estimate of the discretization error. Regarding the tip clearance meshing, 28 layers are refined in the spanwise direction while ensuring y^+ near the unity at tip and shroud.

The model is solved by CFX in the three above mentioned computational domains although the study area is located across the impeller domain. Stationary-rotating interfaces were solved by means of the mixing plane approach. Working fluid properties are characterized using Redlich Kwong equations. The k-ω shear stress transport turbulence model selected, which suits particularly to this application due to its high accuracy and robustness simulating laminar-turbulent flow transition in boundary layers. Regarding the solver control parameters, both high resolution advection scheme and turbulence numerics have been applied. The convergence criterion of the root mean square residuals is set to 10^{-4}.

Tip leakage characterization has been undertaken using control surfaces on the tip gaps of both main and splitter blades. Figure 1 allows the visualization of these tip leakage streamlines over the meshed surface of the blades. Due to these control surfaces, the mass flow leakage computation can be conducted and a clearance leakage mass flow ratio (χ_{cl}) is calculated.

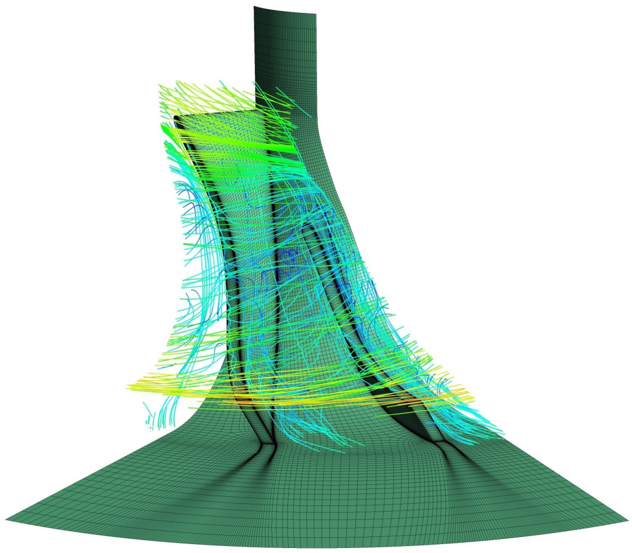

Figure 1: **Visualization of tip leakage velocity streamlines on the meshed geometry.**

$$\chi_{cl} = \frac{Z}{\dot{m}}\left[\int_{lm}^{tm} d\dot{m}_{cl} + \int_{ls}^{ts} d\dot{m}_{cl}\right] \tag{7}$$

Once the leakage mass flow is obtained, the losses due to tip clearance phenomenon can be assessed in relative terms compared to the total input power of the compressor. Hence, their related decrease in efficiency ($-\Delta\eta_{cl}$) is evaluated taking into account the same previous assumption in the analytical methods that all the kinetic energy of the jet is lost (Eq. 8).

$$-\Delta\eta_{cl} = \frac{Z}{\dot{m}(h_{03}-h_{01})}\left[\int_{lm}^{tm} \frac{1}{2}w_{cl,n}^2 d\dot{m}_{cl} + \int_{ls}^{ts} \frac{1}{2}w_{cl,n}^2 d\dot{m}_{cl}\right] \tag{8}$$

RESULTS

This section begins with the analysis of the influence of slight inlet pressurization (1-4 bar) on the analytically predicted tip clearance losses. The selected pressurization range is in line with Valdés et al. (2018) calculations for a future experimentation campaign. Figure 2 shows these predictions according to both Jansen (1967) and Aungier (2000) methods when the reference compressor is using air at three different speedlines near the design rotational speed. The dimensionless mass flow shift due to Re is observed when increasing inlet pressure. In addition, this Re influence also takes places in the asymptotic trend of the clearance loss because of the developed turbulent flow. These values are maintained in the same order of magnitude at the considered rotational speed range. However, an inverse trend can be observed between both methods when increasing the rotational speed.

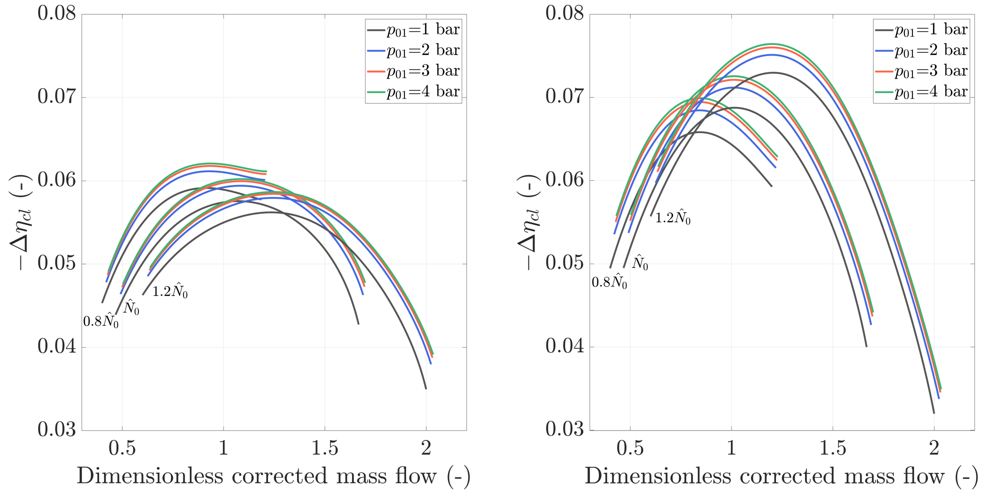

(a) Jansen's method (b) Aungier's method

Figure 2: **Analytical prediction of the efficiency loss due to clearance leakage using pressurized air at different rotational speeds.**

The influence of varying working fluids for different inlet pressures is evaluated in Figure 3 at the design homologous rotational speed, where isobutane pressurization is limited to avoid condensation in the compression stage. Predicted efficiency loss at these conditions is ±5% around those values obtained with air for both methods. The higher Re values when moving to higher density fluids, such as isobutane (Ib.) and propane (Pr.), justify the slight decrease in $\Delta\eta_{cl}$ when pressurizing due to their lower increase in isentropic efficiency. Carbon dioxide behavior represents an intermediate performance, with mild effects of pressurization on $\Delta\eta_{cl}$.

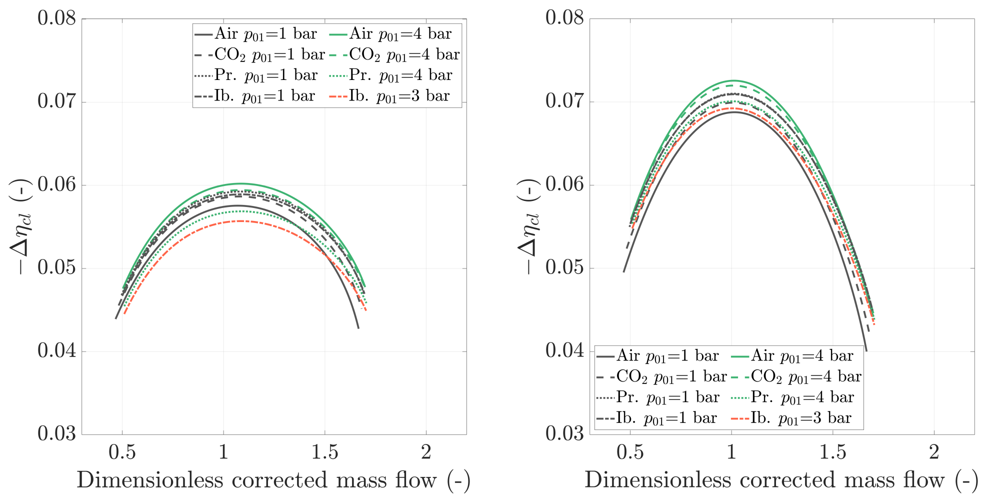

(a) Jansen's method (b) Aungier's method

Figure 3: **Analytical prediction of the efficiency loss due to clearance leakage with different pressurized working fluids at the homologous design speedline.**

Clearance leakage mass flow ratio can be also predicted using Aungier's method. Figure 4 depicts the effect of inlet pressurization on this parameter for the four fluids considered at three homologous rotational speeds. Neither the pressurization nor the working fluid variation involve any variation on χ_{cl} according to analytical results. One may note the sharp increase from 0.15 to almost 0.5 when moving to surge conditions. In addition, numerical results obtained via CFD are also plotted. A good accordance can be observed with the predicted results across almost the whole operating mass flow range except for some divergences near surge. A slight effect of pressurization appears on χ_{cl} at mass flows near choke and surge conditions without modifying the global trend of the line.

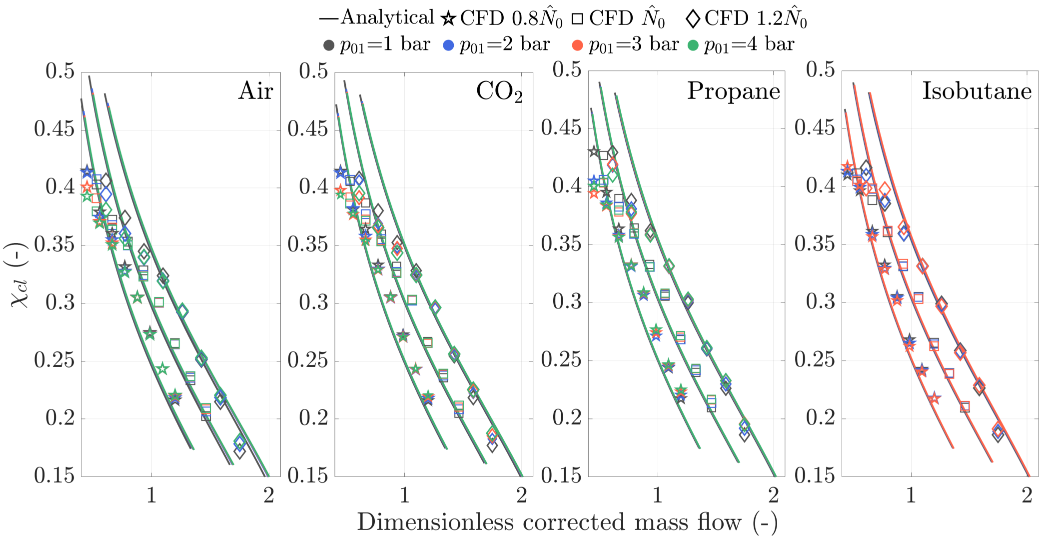

Figure 4: **Clearance leakage mass flow comparison for the considered pressurized fluids at three different rotational speeds.**

In order to take a more thorough analysis of the the effect of pressurization and working fluid variation on clearance leakage losses, two streamwise profiles obtained via CFD are presented in Figure 5. These profiles are captured in the half-span clearance gap of the main and splitter compressor blades. The operating point calculated is at design homologous rotational speed and dimensionless corrected mass flow equal to the unit. For the sake of simplicity, only carbon dioxide and propane behaviors are represented since extrapolated results could be devised for air an isobutane respectively. Figure 5a and 5b depict the relative Mach number (Ma_w) profile. Mild variations of the mentioned profile can be appreciated either varying the fluid or the inlet pressure, being more significant in the splitter blade. However, the characteristic pattern is maintained, showing the higher values at the inducer and tip locations. Therefore, it can be stated that the increase in pressure difference due to inlet pressurization between pressure and suction sides of the blades does not convey an increase in Ma_w.

Jet density profile is also presented in comparison to the inlet total density (ρ/ρ_{01}) for the same previous selected cases at the main and splitter blades (Figure 5c and 5d). The pattern of the profile shows lower densities near the trailing edge and a successive increase along the blade. Maximum values are obtained at the leading edge of both blades, where high relative velocities are also found. The effect of varying working fluid and inlet pressurization can be better appreciated near 0.6 and 0.9 values of the streamwise relative location. These zones coincide with both the low Ma_w peak and their increase near the leading edge. Differences up

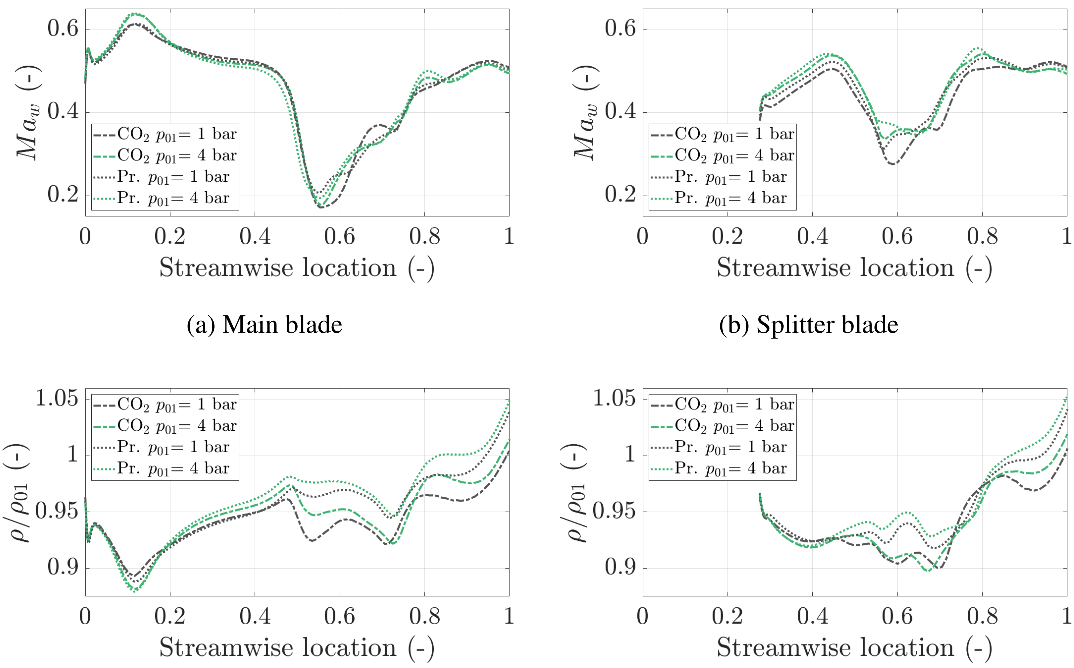

(a) Main blade

(b) Splitter blade

(c) Main blade

(d) Splitter blade

Figure 5: **Relative Mach number (a, b) and dimensionless jet density (c, d) profiles at the half-span clearance gap.**

to 5 percentage points are found while the global profile pattern is maintained.

Finally, numerical calculated efficiency variations due to clearance losses are shown in Figure 6, where all the selected cases (fluids, pressurization and rotational speeds) are plotted. One may point out the remarkable difference in magnitude in comparison to the previously analytically obtained results in Figs 2-3. In addition, a monotonous increase in $\Delta\eta_{cl}$ can be appreciated instead of the efficiency loss global maximum predicted. These discrepant results reaffirm those analytical prediction methods limitations for small-scale compressors with large tip clearance ratios. Furthermore, the order of magnitude and shape of the obtained values are in line with recent studies where $\Delta\eta_{cl}$ to relative clearance ratios near the unity are obtained at high mass flow conditions (Diehl et al., 2020).

Similar efficiency variations due to clearance losses are obtained for the four working fluids. These values are also maintained along the three rotational speeds considered. It should be reminded that their operational conditions are adapted according to dynamical similarity and Re correction. This common efficiency drop could be nearly tripled from near surge to near choke conditions. Hence, the higher mass flow conditions involve higher tip leakage losses in spite of the leakage mass flow decrease. The quadratic effect of relative velocity is, therefore, dominating this phenomenon when assuming that all this kinetic energy is lost.

As it was anticipated, the effect of inlet pressurization is almost negligible in the proposed calculation space. The slight variations of the tip jet density or relative velocity do not involve a noteworthy increase in $\Delta\eta_{cl}$. In other words, increasing four times the inlet design atmospheric pressure does not convey notably higher tip clearance losses. Furthermore, it could also be underlined the absence of variations due to specific heat ratio among the considered fluids.

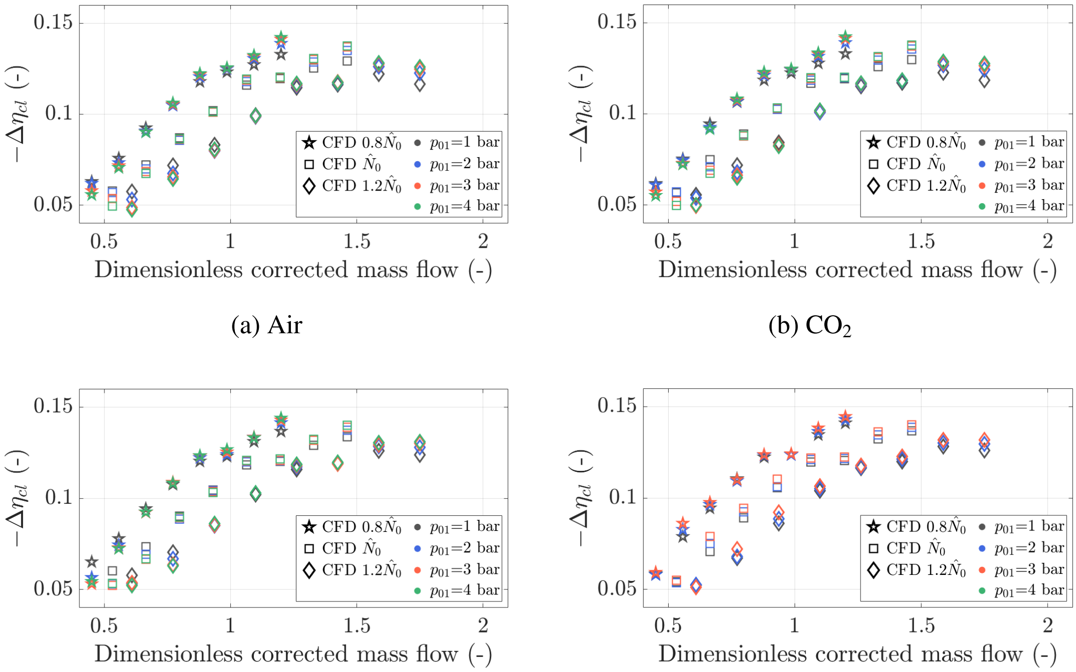

(a) Air (b) CO_2

(c) Propane (d) Isobutane

Figure 6: **Numerically calculated efficiency drop due to tip leakage for the considered working fluids, inlet pressure range and rotational speed.**

CONCLUSIONS

The present study investigates the effect of pressurization on tip clearance losses in micro-scale centrifugal compressors. This pressurization is motivated by the use of different working fluids in closed-loop conditions, which can devise beneficial effects on compressor efficiency due to Reynolds-number increases. Tip clearance leakage phenomenon has been characterized by means of both analytical and numerical methods when the compressor is running in off-design conditions.

In light of the results of this research, both methods agree in the fact that increasing inlet pressure has low or even negligible influence on the clearance leakage related efficiency drop. Notable differences in magnitude are found between them, leading to reaffirm the limitations of the selected prediction methods for these small machines with large clearance ratios. Numerical results also show the tip clearance loss independence related to the working fluids variation, which supports their Reynolds-number independence and a negligible effect of the specific heat ratio. In addition, the tip leakage flow structure is preserved in the pressure range investigated because the tip jet relative Mach number and density profiles hardly change. Therefore, the beneficial effects of Reynolds-number increase in the laminar-to-turbulent regime on efficiency may not be countered by eventual tip clearance losses.

ACKNOWLEDGEMENTS

This research has been supported by the Spanish *Ministerio de Ciencia e Innovación* under the project of reference number PID2019-110283RB-C32.

REFERENCES

Aungier, R. (2000). *Centrifugal Compressors: A Strategy for Aerodynamic Design and Analysis*. Number v. 10. ASME Press.

Casey, M., Krähenbuhl, D., and Zwyssig, C. (2013). The design of ultra-high-speed miniature centrifugal compressors. In *Proceedings of the 10th European Conference on Turbomachinery, Fluid Dynamics and Thermodynamics*.

Demierre, J., Henchoz, S., and Favrat, D. (2012). Prototype of a thermally driven heat pump based on integrated organic rankine cycles (orc). *Energy*, 41(1):10 – 17. 23rd International Conference on Efficiency, Cost, Optimization, Simulation and Environmental Impact of Energy Systems, ECOS 2010.

Diehl, M., Schreiber, C., and Schiffmann, J. (2020). The Role of Reynolds Number Effect and Tip Leakage in Compressor Geometry Scaling at Low Turbulent Reynolds Numbers. *Journal of Turbomachinery*, 142(3). 031003.

Dietmann, F. and Casey, M. (2013). The effects of reynolds number and roughness on compressor performance. In *Proceedings of the 10th European Conference on Turbomachinery, Fluid Dynamics and Thermodynamics*.

İlhan, M., Gürbüz, M. T., and Acarer, S. (2019). Unified low-pressure compressor concept for engines of future high-speed micro-unmanned aerial vehicles. *Proceedings of the Institution of Mechanical Engineers, Part G: Journal of Aerospace Engineering*, 233(14):5264–5281.

Jaatinen-Värri, A., Tiainen, J., Turunen-Saaresti, T., Grönman, A., Ameli, A., Engeda, A., and Backman, J. (2016). Centrifugal compressor tip clearance and impeller flow. *Journal of Mechanical Science and Technology*, 30(11):5029–5040.

Jansen, W. (1967). A method for calculating the flow in a centrifugal compressor impeller when entropy gradients are present. *In: Royal Society conference on internal aerodynamics (turbomachinery)*, pages 133–146.

Kim, C., Lee, H., Yang, J., Son, C., and Hwang, Y. (2016). Study on the performance of a centrifugal compressor considering running tip clearance. *International Journal of Refrigeration*, 65:92–102.

Sebastián, A., Abbas, R., Valdés, M., and Rovira, A. (2021). Modular micro-trigeneration system for a novel rotatory solar fresnel collector: A design space analysis. *Energy Conversion and Management*, 227:113599.

Valdés, M., Sebastián, A., and Abbas, R. (2018). Reynolds-number-dependent efficiency characterization of a micro-scale centrifugal compressor using non-conventional working fluids. *Energy Conversion and Management*, 177:224 – 232.

Wang, H., Xi, G., Li, J., and Yuan, M. (2011). Effect of the tip clearance variation on the performance of a centrifugal compressor with considering impeller deformation. *Proceedings of the Institution of Mechanical Engineers, Part A: Journal of Power and Energy*, 225(8):1143–1155.

Zhao, D., Daniel, K., Blunier, B., Zwyssig, C., Dou, M., and Miraoui, A. (2012). Design and control of an ultra high speed turbo compressor for the air management of fuel cell systems. In *Transportation Electrification Conference and Expo (ITEC)*, pages 1–6. IEEE.